INTERNATIONAL JOURNAL OF
Minerals, Metallurgy and Materials

Volume 31, Number 6, June 2024
Page 1228

Research Article https://doi.org/10.1007/s12613-023-2693-7

# Process metallurgy and data-driven prediction and feedback of blast furnace heat indicators

*Quan Shi*[1,2,3], *Jue Tang*[1,2,3],✉, *and Mansheng Chu*[1,2,3],✉

1) School of Metallurgy, Northeastern University, Shenyang 110819, China
2) Institute for Frontier Technologies of Low-carbon Steelmaking, Northeastern University, Shenyang 110819, China
3) Engineering Research Center of Frontier Technologies for Low-carbon Steelmaking (Ministry of Education), Shenyang 110819, China

(Received: 27 March 2023; revised: 6 June 2023; accepted: 16 June 2023)

**Abstract:** The prediction and control of furnace heat indicators are of great importance for improving the heat levels and conditions of the complex and difficult-to-operate hour-class delay blast furnace (BF) system. In this work, a prediction and feedback model of furnace heat indicators based on the fusion of data-driven and BF ironmaking processes was proposed. The data on raw and fuel materials, process operation, smelting state, and slag and iron discharge during the whole BF process comprised 171 variables with 9223 groups of data and were comprehensively analyzed. A novel method for the delay analysis of furnace heat indicators was established. The extracted delay variables were found to play an important role in modeling. The method that combined the genetic algorithm and stacking efficiently improved performance compared with the traditional machine learning algorithm in improving the hit ratio of the furnace heat prediction model. The hit ratio for predicting the temperature of hot metal in the error range of ±10°C was 92.4%, and that for the chemical heat of hot metal in the error range of ±0.1wt% was 93.3%. On the basis of the furnace heat prediction model and expert experience, a feedback model of furnace heat operation was established to obtain quantitative operation suggestions for stabilizing BF heat levels. These suggestions were highly accepted by BF operators. Finally, the comprehensive and dynamic model proposed in this work was successfully applied in a practical BF system. It improved the BF temperature level remarkably, increasing the furnace temperature stability rate from 54.9% to 84.9%. This improvement achieved considerable economic benefits.

**Keywords:** blast furnace; furnace heat; genetic algorithm; stacking; prediction and feedback

## 1. Introduction

Inner blast furnaces (BFs) cannot be directly monitored. Instead, their heat levels are represented by the physical heat (temperature) and chemical heat ([Si]) of hot metal. The temperature and [Si] of hot metal are associated with energy utilization and are important indices for judging the quality of pig iron. Their range and frequency of variation can also reflect the stability of the production process [1–2]. Extremely high or low furnace temperatures will cause not only the unqualified quality of hot metal but also fluctuations in furnace conditions and even abnormal accidents [3–6]. During traditional BF production, heat levels are estimated by observing the brightness and shape of hot metal and the appearance of condensed pig iron. Then, the furnace heat level and condition are judged by combining the change in temperature measurement and personal experience. However, the magnitude of error from different operators will influence the adjustment strategy. In addition, although the laboratory analysis of [Si] is highly accurate, its results are obtained after half an hour, which can reduce their reference value for actual BF production and prevent the timely discovery of excessive [Si] and adjustment of operating parameters to correct furnace heat levels, resulting in massive losses. Accurately predicting furnace heat levels and adjusting BFs in advance in accordance with the feedback operation suggestion inferred from forecasted results are of great importance because they are beneficial to ensure the smooth smelting and economic benefit of BF ironmaking.

Big data technology has become widely applied in ironmaking and steelmaking with the development of digital transformation in the steel industry [7–11]. Furnace heat prediction is becoming an important part of intelligent BF ironmaking technology, and some data-driven modeling methods focusing on furnace heat indicators have been proposed. Considering the complexity of BF smelting and the numerous parameters that affect furnace heat, high-dimensional data are not conducive to the establishment of a heat model; principal component analysis (PCA) is often used to reduce the dimension of BF parameters [12–14]. However, PCA considers only the correlation among input variables but not those between input and output variables. Given their high efficiency, the Pearson, Spearman, and maximal information coefficient (MIC) methods are often used to screen charac-

✉ Corresponding authors: Jue Tang E-mail: tangj@smm.neu.edu.cn; Mansheng Chu E-mail: chums@smm.neu.edu.cn

teristics with a strong correlation with furnace heat indices [15–17]. Many scholars have conducted research on furnace heat prediction. Zhou *et al.* [18] established the prediction models of the temperature and [Si] of hot metal based on the recursive subspace identification method. In this method, the parameters of the prediction model were adaptively updated by using the latest BF process data to ensure the accurate prediction of furnace heat levels. Li and Yang [19] utilized the genetic algorithm (GA) framework and ironmaking knowledge to construct explainable features and achieved high accuracy in [Si] prediction. Jiang *et al.* [20] predicted [Si] by using an attention-wise deep transfer network and described the dynamic relationship between input and output. Such an approach was conducive to improving the comprehensibility and transparency of the prediction results. Li *et al.* [21–23] studied a series of multi-input multioutput models for the prediction of BF heat indicators on the basis of the Takagi–Sugeno fuzzy model and random vector functional link networks. The advantage of this series of models was that the correlation between the output indices of hot metal was considered, and model accuracy was improved effectively.

Although considerable research has been done on the prediction of furnace temperature indicators, some areas still need improvement. For example, the dimension and quantity of modeling data are not considered comprehensively, the time delay analysis and modeling methods are inadequately combined with the BF process, and real application scenarios for verification are lacking. When predicting and optimizing BF heat levels, the process principle of material and heat balances should be followed, and the complex random fluctuations in actual smelting conditions and reaction processes should be considered completely. A model combining the process and algorithm must be established, verified, and optimized constantly in production practice [24]. In this work, a model for the prediction and feedback of furnace heat indicators was established on the basis of the fusion of data-driven and BF processes and successfully applied to an ongoing BF in China with remarkable benefits. The rest of this paper is organized as follows: The model-building approach is explained in detail in section 2. The proposed method was validated on a BF dataset, and the results are discussed in section 3. The performance of the model in an industrial application is shared in section 4. Finally, the conclusion is drawn.

## 2. Methodology

The general technical route of this work is presented in Fig. 1. This work has five parts as follows: big data preprocessing and dimension reduction, time lag analysis, furnace heat prediction model, furnace heat feedback model, and online application.

### 2.1. BF data preprocessing and dimension reduction

2.1.1. BF data collection and preprocessing

The data in this work were derived from the practical production data of a domestic BF taken over 1 year. The collected data were sorted in accordance with the whole BF smelting process and comprised raw and fuel, process operation, smelting condition, and slag and iron discharge data with a total of 171 variables. The detailed data classification is shown in Table 1. In data preprocessing, the deletion and filling methods were applied to process missing values. Outliers were identified and treated by the box diagram method combined with BF operating guidelines. All the data of different frequencies were converted into hourly frequencies to

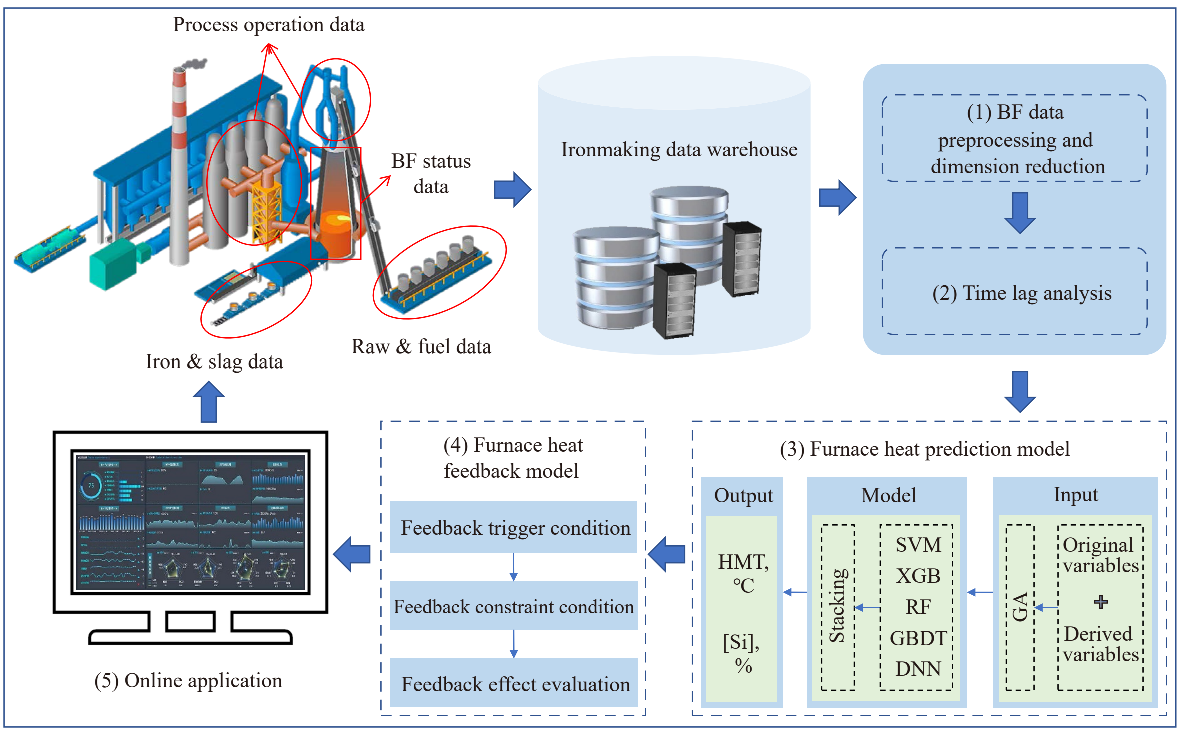


**Fig. 1. General technical route of this work.**

**Table 1. Collection and classification of BF data**

| Class | Amount | Frequency / h | Feature names |
|---|---|---|---|
| Sintering data | 9 | 2 | Sintering composition, size, quality, and metallurgical properties |
| Pellet data | 9 | 2 | Pellet composition, size, quality, and metallurgical properties |
| Coke data | 10 | 4 | Coke composition, size, quality, and metallurgical properties |
| Coal data | 7 | 4 | Coal composition and calorific value |
| BF operation data | 17 | 1 | Raw fuel ratio and consumption, burden distribution parameters, blast parameters, coal injection parameters, cooling water parameters, and speed of material descent |
| BF status data | 108 | 1 | Furnace top pressure, total differential pressure, furnace top temperature, gas utilization rate, breathability, thermocouple temperature, heat flow intensity, and water temperature |
| Iron & slag data | 11 | Frequency of hot metal | Iron batch number, hot metal composition, slag composition, and amount of iron and slag from different iron notches |

solve the problem of unbalanced data samples caused by different data acquisition cycles in different processes. The detailed data processing methods are shown in Table 2. After data preprocessing, 9223 sets of hourly frequency sample data were obtained.

2.1.2. Dimension reduction of BF data

BF system data were classified as high-dimensional data. The collinearity test, the integration of the same type of parameters, and correlation analysis were used to reduce the dimensions of BF data for the preliminary screening of input variables. For example, the parameter of high collinearity between BF parameters was eliminated, and the mean value, range, and standard deviation of the temperature of the cooler at the same height in the circular direction were calculated instead of the temperature parameters of the original measuring point. Some variables that were irrelevant or weakly correlated with furnace heat indicators were removed through the MIC method. As a result, the number of BF parameters decreased from 171 variables to 77 variables.

### 2.2. Time delay analysis of BF data

2.2.1. Process modeling

During ironmaking, a specific operational measure takes effect after a certain period of time following its implementation. The lag time of each related variable of the furnace heat indicator differs. In general, the purpose of the existing time delay analysis is to determine the specific time delay through correlation analysis [25–26], which has a certain one-sidedness. As a result of different furnace conditions, the lag time and influence degree of related variables on furnace heat indicators are not fixed but instead change within a certain range. As shown in Fig. 2, First, the upper and lower limits of the lag time were determined. Based on the smelting cycle of the BF studied, 0 and 6 h were used as the upper and lower limits of the lag time. Second, the lag times of the related variables in different time periods were calculated. By comprehensively considering the frequency of the actual material changes in the blast furnace and the expert recommendations, it is more appropriate to differentiate the blast furnace conditions based on the monthly frequency. Therefore, in this study, the data were divided into twelve monthly segments; the time lag was analyzed separately for each month, and the combined set was used to determine the lag time. Third, the lag-time range for each parameter was calculated. The lag time of each parameter was counted for all time periods, and the maximum and minimum lag times were used as the time-lag ranges for that parameter. Finally, this method obtained multiple lag times, which were constructed as new delay-derived features. For example, the lag times for variable $x$ from June to December were 1, 2, 2, 2, 1, 1, and 2 h respectively. The final lag times for variable $x$ were then 1 and 2 h. Both $x$ before 1 h ($x^{-1}$) and 2 h ($x^{-2}$) were treated as new features and employed in the feature selection process of the model. Incorporating the time-lag information of the variables into the model can result in a more rational model and better modeling results.

2.2.2. Analysis of results

Considering that the number of variables after preliminary filtering was still large, cold air flow was taken as an example, and the analysis results of time delay are shown in Fig. 3. The change in the effect of the maximum information coefficient of cold air flow rate on furnace heat indicators with a lag of 1–6 h was analyzed by taking the value of cold air flow rate at the current moment (0 h) as the reference value. The effect of cold air flow rate on furnace heat indicators in each period first increased and then decreased, indicat-

**Table 2. Preprocessing of BF data**

| Type | Method | Description |
|---|---|---|
| Missing data processing | Delete & fill | Delete: missing data (<5%) or (>30%)<br>Fill: intermittent short-term loss of data (interpolation) or long-term loss of data continuity (machine learning) |
| Outlier data processing | Box plot & operating guidelines | Delete or correct or treat as a missing value |
| Mixed frequency data processing | All converted into hourly frequency data | High-frequency data were averaged or summed in accordance with the period of low-frequency data, and low-frequency data were mapped to the high-frequency time index |

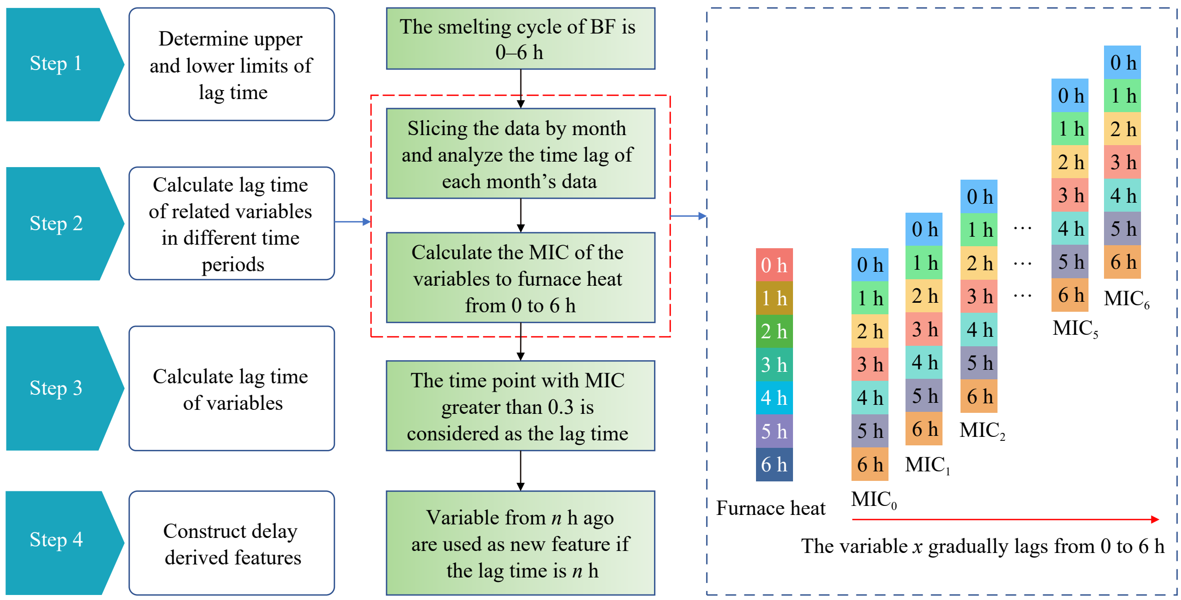


**Fig. 2. Time lag analysis of furnace heat indicators.**

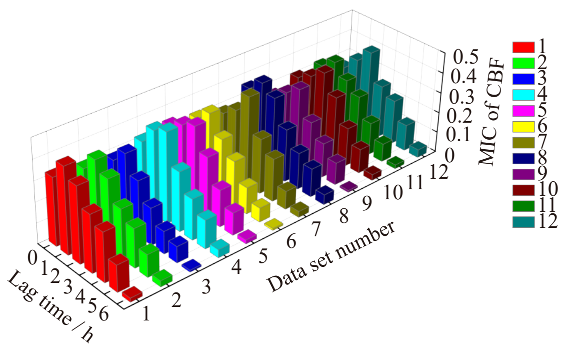


**Fig. 3. Time delay analysis results of CBF.**

ing that the effect of cold air flow rate on the furnace heat index had a lag. The effect of the cold air flow rate on the furnace heat indicator when the lag time was 1 or 2 h was significantly higher than that at other times, illustrating that the lag time of the cold air flow rate ranged from 1 to 2 h. Therefore, $CBF^{-1}$ and $CBF^{-2}$ were added as the input variables of the furnace heat prediction model. The time delay analysis results of other relevant variables are presented in Table 3. Only a part of the results was listed in Table 3 due to the large number of variables. After the time delay analysis, 52 variables were extracted as the candidate variables for model input.

## 3. Results and discussion of furnace heat indicator prediction and feedback

The current furnace heat level can be obtained by observing, testing iron samples or measuring temperature and, more importantly, used to predict the future furnace heat level. In this work, the average temperature of hot metal and [Si] in the next 1 h was selected for prediction.

### 3.1. Utilization of the furnace heat index model

Numerous studies on furnace heat indicators have been conducted [27–29], and the theoretical calculation of furnace heat indicators can be performed by using the heat balance and carbon–oxygen balance equations. However, due to the lack of modification of smelting data, a certain deviation exists between the theoretical calculation results and actual measured values. On the basis of the furnace heat index model, theoretical calculation variables, such as the slag and iron heat indices, direct reduction degree, and fuel ratio deviation, were used as the input variables in the furnace heat indicator prediction model to exploit the information provided by the mechanism model to compensate for the shortage of monitoring means in actual production.

**Table 3. Results of the lag time analysis of relevant variables**

| Related variables | Symbol | Time lag |
|---|---|---|
| Cold blast flow | CBF | $CBF^{-1}$, $CBF^{-2}$ |
| Hot blast temperature | HBT | $HBT^{-1}$ |
| Hot blast pressure | HBP | $HBP^{-1}$, $HBP^{-2}$ |
| Pressure difference | PD | $PD^{-1}$, $PD^{-2}$ |
| Gas permeability | GP | $GP^{-1}$, $GP^{-2}$ |
| Top blast temperature | TBT | $TBT^{-1}$ |
| Top blast pressure | TBP | $TBP^{-1}$ |
| Oxygen enrichment flow | OEF | $OEF^{-1}$, $OEF^{-2}$ |
| Theoretical combustion temperature | TCT | $TCT^{-1}$, $TCT^{-2}$ |
| Bosh gas volume | BGV | $BGV^{-1}$, $BGV^{-2}$ |
| Pulverized coal injection | PCI | $PCI^{-1}$, $PCI^{-2}$, $PCI^{-3}$ |
| Coke consumption | CC | $CC^{-1}$, $CC^{-2}$, $CC^{-3}$ |
| Sinter basicity | SB1 | $SB1^{-1}$, $SB1^{-2}$, $SB1^{-3}$ |
| … | … | … |

### 3.2. Selection of furnace heat features based on GA

3.2.1. Process modeling

The initial input variable set of the model for the prediction of furnace heat indicators comprised the variables of initial filtration obtained through correlation analysis, the newly created variables based on lag time, and the derived variables based on the slag and iron heat index model. However, not all variables are required by the model. GA is an effective feature selection method that can screen out the optimal feature combination in the case of a large number of features and improve model performance [30–31]. In this study, GA was used to further reduce the dimension of the initial input variables and screen the optimal feature combination when the accuracy of the heat index prediction model was the highest. This process included the six steps shown in Fig. 4. First, the initial population was generated, and the fitness function was defined. Subsequently, roulette selection [32], crossover, and mutation were performed, followed by the combined evaluation of new individuals. Finally, the optimal feature combination was selected and returned.

3.2.2. Model input determination

Correlation, time delay, and slag and iron heat index analyses provided a large number of input variables for the furnace heat prediction model. In this work, the above method was adopted to further reduce the dimension of the initial input variables, and the variables in Table 4 were finally identified as the input. Given that the smelting of BF is continuous and uninterrupted, the previous heat level has a certain influence on the next heat level. Therefore, the historical temperatures of hot metal and [Si] were added to the model.

### 3.3. Furnace heat prediction model based on stacking

3.3.1. Process modeling

The choice of predictor is crucial for model performance. In this work, an integrated learning strategy based on the stacking framework was used to predict the furnace heat indicators accurately. The technical route is given in Fig. 5. Different algorithms were integrated by the stacking framework, and their observations of different data from different spaces and structures were efficiently applied to optimize stacking results [33]. Finally, five base learners, including

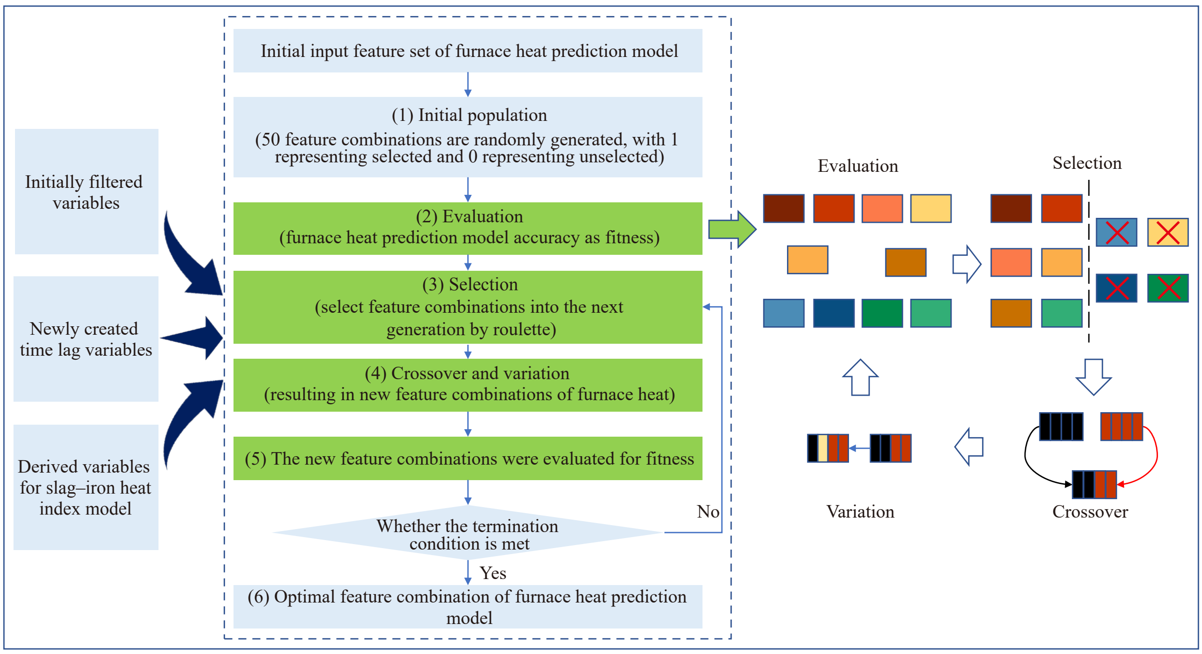


**Fig. 4. Feature selection process based on GA.**

**Table 4. Optimal feature combination for the model**

| Feature name | Symbol | Feature name | Symbol |
|---|---|---|---|
| Temperature of hot metal | HMT, $HMT^{-1}$ | Sinter $SiO_2$ | $SSi^{-2}$ |
| [Si] of hot metal | [Si], $[Si]^{-1}$ | Coke FCad | CFC1 |
| Hot blast pressure | HBP, $HBP^{-1}$, $HBP^{-2}$ | Coal FCad | CFC2 |
| Gas permeability | GP | Gas utilization rate | GUR |
| Heat load | HL | Theoretical coke ratio | TCR1 |
| Top blast temperature | TBT, $TBT^{-1}$ | Theoretical coal ratio | TCR2 |
| Oxygen enrichment flow | OEF, $OEF^{-1}$, $OEF^{-2}$ | Burden descent speed | BDS |
| Theoretical combustion temperature | $TCT^{-1}$ | Slag iron heat index | $SIHI^{-1}$, $SIHI^{-2}$ |
| Bosh gas volume | $BGV^{-1}$ | Direct reduction degree | DRD, $DRD^{-2}$ |
| Pulverized coal injection | PCI, $PCI^{-1}$, $PCI^{-2}$ | Fuel ratio deviation | FRD, $FRD^{-1}$ |
| Coke consumption | CC, $CC^{-1}$, $CC^{-2}$ | Slag basicity | SB2 |
| Cold wind flow | $CBF^{-1}$ | Slag amount | SA |
| Sinter basicity | $SB1^{-2}$ | Theoretical iron quantity | TIQ |

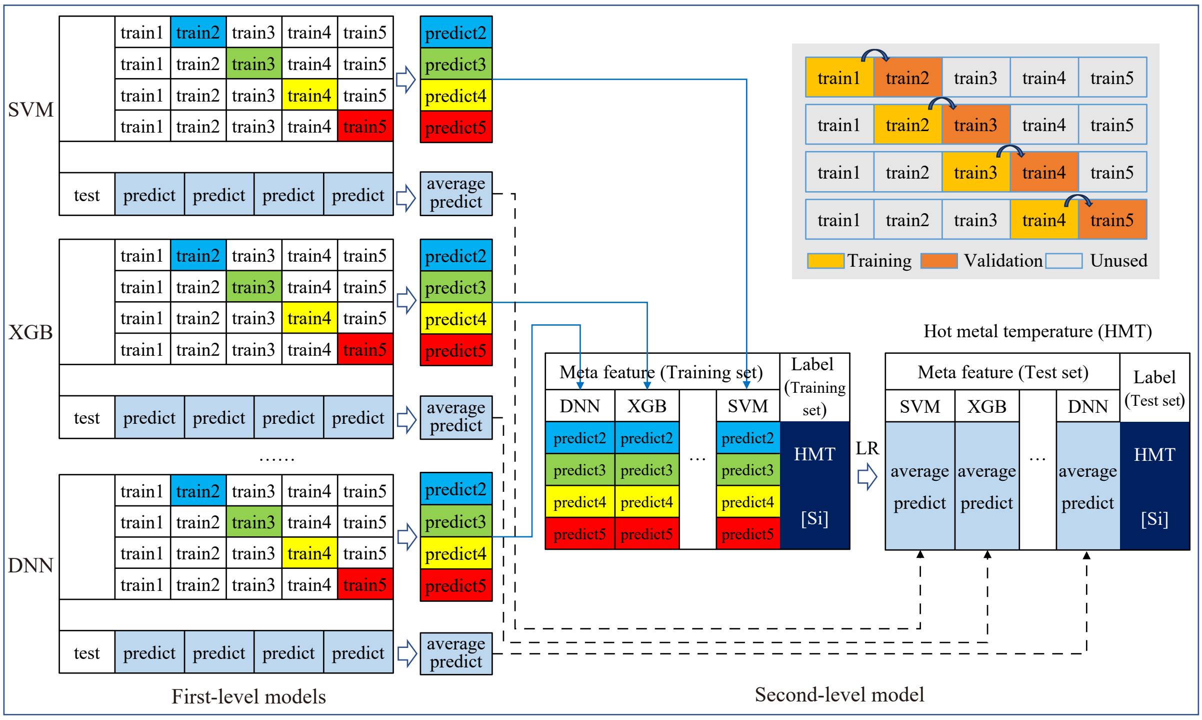


**Fig. 5. Prediction model of furnace heat indicators based on the stacking framework.**

support vector machine (SVM), extreme gradient boosting (XGB), random forest (RF), gradient boosting decision tree (GBDT), and deep neural network (DNN), were selected as the first layer model. A simple linear regression (LR) model was selected as the second-layer model for modeling and prediction to reduce the overfitting risk. However, directly using the model obtained by training the training set to predict the labels of the training set carries a high risk of overfitting. Therefore, cross-validation was selected to mitigate the overfitting problem in this approach. In this study, we used sliding time-series cross-validation and not the standard k-fold cross-validation when dealing with time-series data. First, the time series was divided into five consecutive and equal numbers of data blocks according to the time series, and no random splitting was used. These five data blocks were labeled as train1 through train5. Second, each data block was used for model testing and retraining, whereas data block train1 is used only for training. For example, we trained the model using data block train1, used it to predict data block train2, and subsequently continued this process by training the model with each subsequent data block, predicting the next one, and so forth until data block train5 is predicted. Finally, the predictions from train2 to train5 were concatenated and used as the output of the primary learner in the training set. This approach discards 1/5 of the data but can mitigate the risk of overfitting caused by directly using the model trained on the training set to predict the labels of the same training set. During the four-fold cross-validation, the test dataset was predicted in each iteration. The mean of the results of these four predictions was used as the output for the primary learner in the test dataset. After each primary learner was trained, a new column of the dataset was generated, and this new dataset was used as a meta-feature. Five primary learners were selected; therefore, five columns of meta-features were generated and used as inputs for the second-layer training model. Similarly, five columns of meta-features were generated after the test set was transformed into stacks as inputs to the second-layer test model. Finally, a linear regression model was used to retrain these meta-features, and a model from the meta-features to the ground -truth was obtained.

3.3.2. Analysis of prediction results

(1) Splitting of the dataset.

The purpose of this work is to predict the temperature of hot metal and [Si] in the next 1 h. In contrast to regression analysis prediction, time-series prediction cannot be randomly divided into training and test sets. Therefore, it is usually divided in accordance with the time sequence of data. The accuracy of the prediction model will be inflated because the data distribution of the randomly divided training and test sets is similar. Therefore, the dataset was divided into two groups, with the first 9055 datasets as the training set and the last 168 datasets as the test set. The splitting of the time-series dataset of furnace heat indicators is shown in Fig. 6. The data to the left of the red line are for training, and those to the right of the red line are for testing. In consideration of some uncertainty in the algorithm, all of the following simulations were run 20 times and then averaged.

(2) Prediction results of the furnace heat indicator.

On the basis of the actual production condition of the BF in this work, the temperature of hot metal was determined to be ±10°C, and [Si] was determined to be ±0.1wt%, which was the hit ratio of the furnace heat prediction model. The test results of temperature and [Si] are shown in Figs. 7 and 8, respectively. The blue lines in Figs. 7(a) and 8(a) respectively represent the actual values of the hot metal temperature and [Si], whereas the red lines represent the predicted values

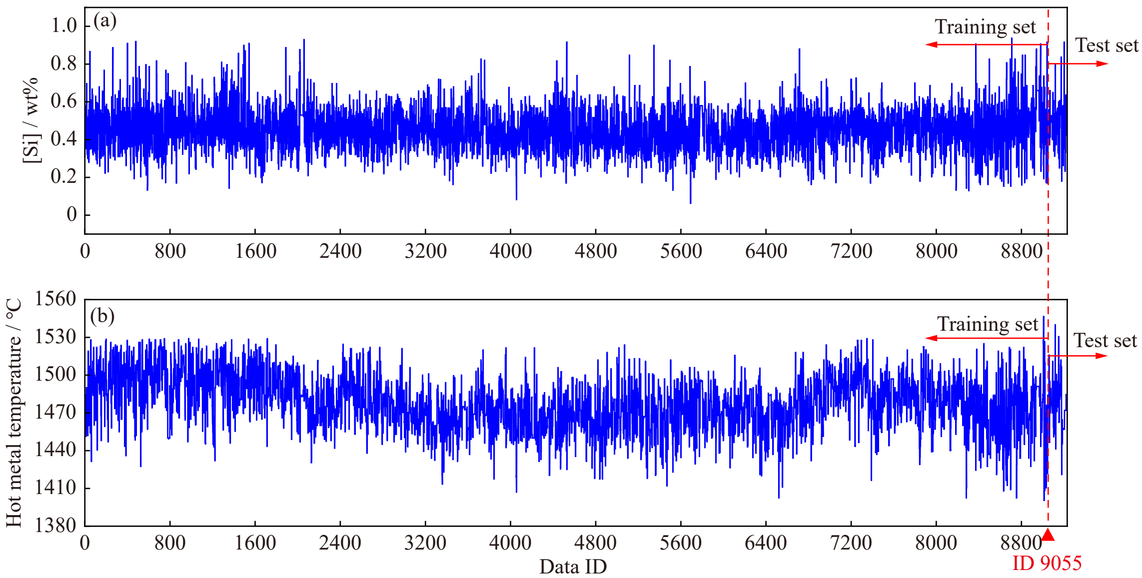


**Fig. 6. Division of training and test sets for [Si] (a) and hot metal temperature (b).**

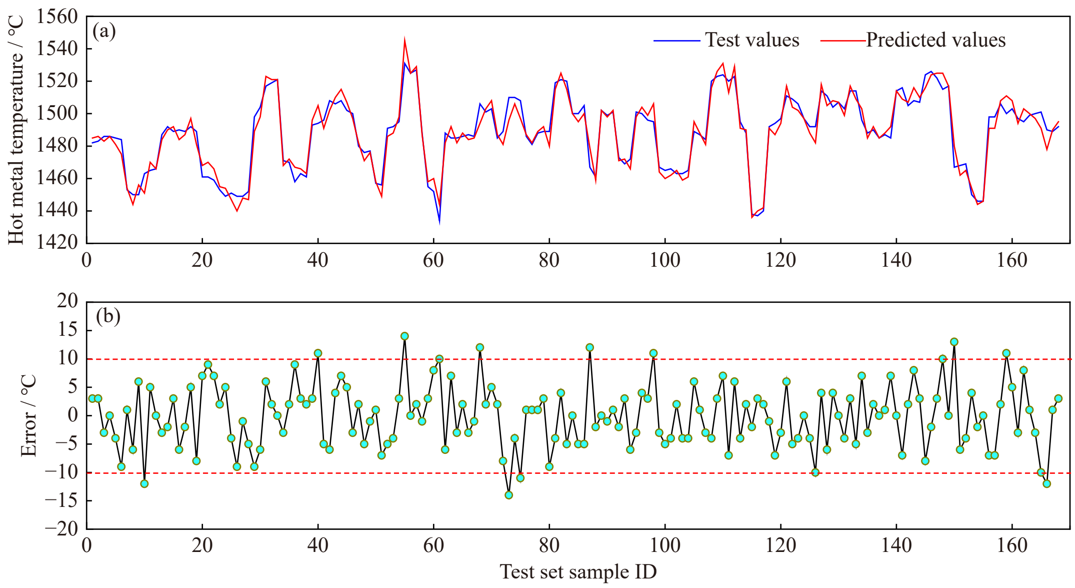


**Fig. 7. Results (a) and error (b) of hot metal temperature prediction.**

by the model established by the algorithm in this work. The coincidence between the real and predicted values was smooth. The dots in Figs. 7(b) and 8(b) respectively represent the difference between the real and predicted values. The residual distribution range of furnace heat indicators was small and concentrated. The residual temperature of hot metal was mainly distributed between −10 and +10°C, and [Si] was mostly distributed between −0.1wt% and +0.1wt%. These distributions can meet the requirement of practical production.

(3) Comparison of the performances of different algorithms.

The test results of the furnace heat indicators provided by different algorithms were compared, as shown in Figs. 9 and 10, to illustrate the hit ratio of the method proposed in this work. Clearly, the method presented in this work had the best performance. The prediction error curves of the probability density function (PDF) of temperature and [Si] provided by the other five algorithms are depicted in Figs. 9(b) and 10(b), respectively, to facilitate comparison. The estimation error of the proposed algorithm was evidently small and concentrated. Figs. 9(c) and 10(c) show the hit ratios of the temperature and [Si] of hot metal provided by different methods, respectively. The hit ratios of the proposed algorithm were 92.4% and 93.3%, which were obviously better than those of other algorithms.

### 3.4. Feedback model of BF heat operation

#### 3.4.1. Process modeling

During ironmaking, the operator must predict the furnace heat accurately through the change in the relevant furnace condition parameters and take reasonable adjustment measures in time. Such an approach is highly beneficial for reducing the fluctuation in furnace conditions and improving the quality of hot metal. Although some optimization methods based on the GA and particle swarm optimization algorithm

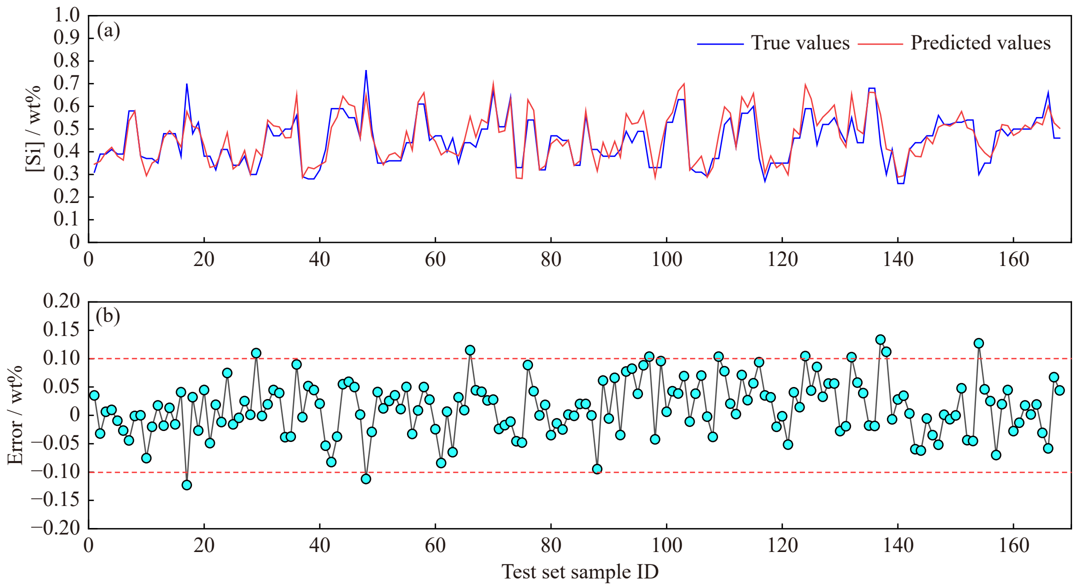


**Fig. 8. Results (a) and error (b) of [Si] prediction.**

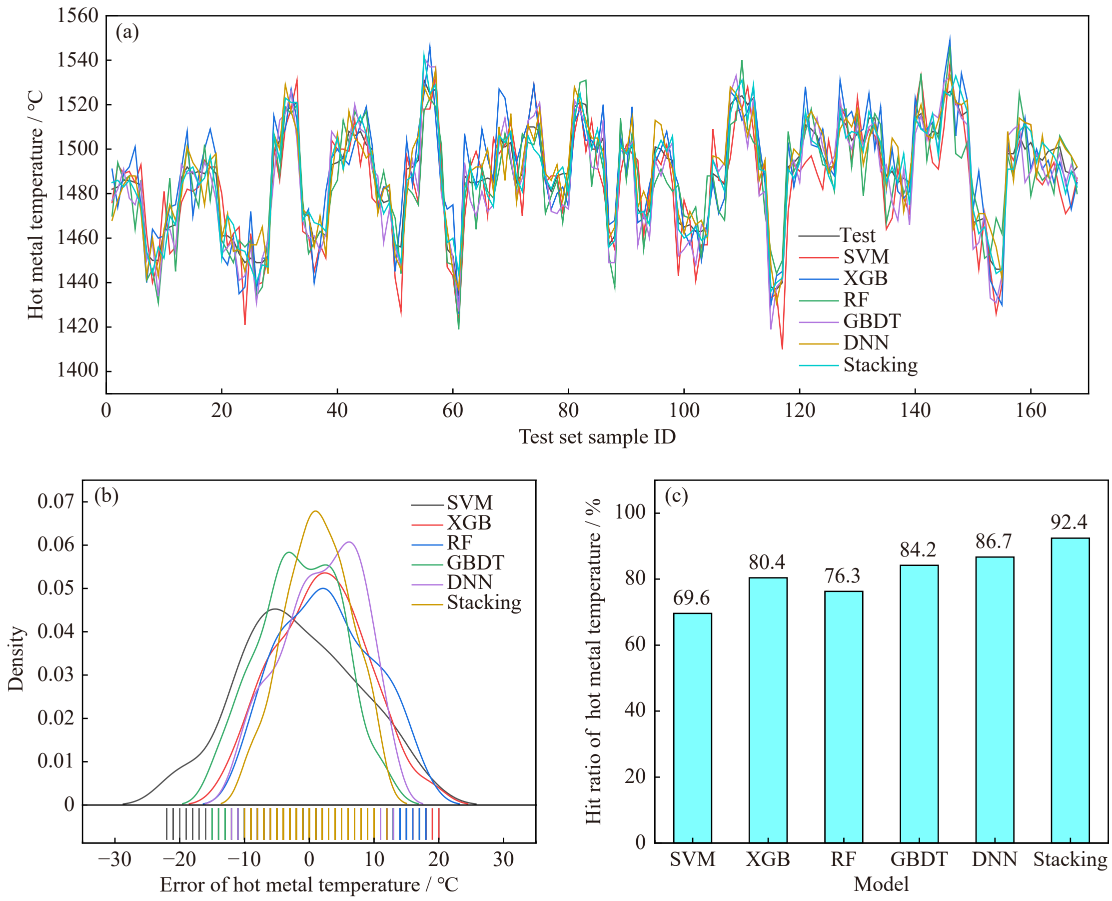


**Fig. 9. Results (a), probability density function (b), and hit ratio (c) of hot metal temperature prediction by different methods.**

have been proposed [34–35], they have excessively long and complicated calculation processes that are unconducive to online applications. Therefore, a feedback model of BF operation with a quick response was established on the basis of the above prediction model. The total time of prediction and feedback was within 5 min, which provided sufficient time to operate the BF and adjust the abnormal furnace heat. When the predicted furnace heat indicator at the next moment reached the feedback triggering condition, the feedback model was triggered, and the operation adjustment plan was pushed to the operator. This situation is beneficial for improving the heat state of the BF and stable production.

The feedback model of operation was divided into three parts, as seen in Fig. 11. In the first part, the feedback trigger condition was set. The threshold values of the furnace heat indicators were set in accordance with the actual production

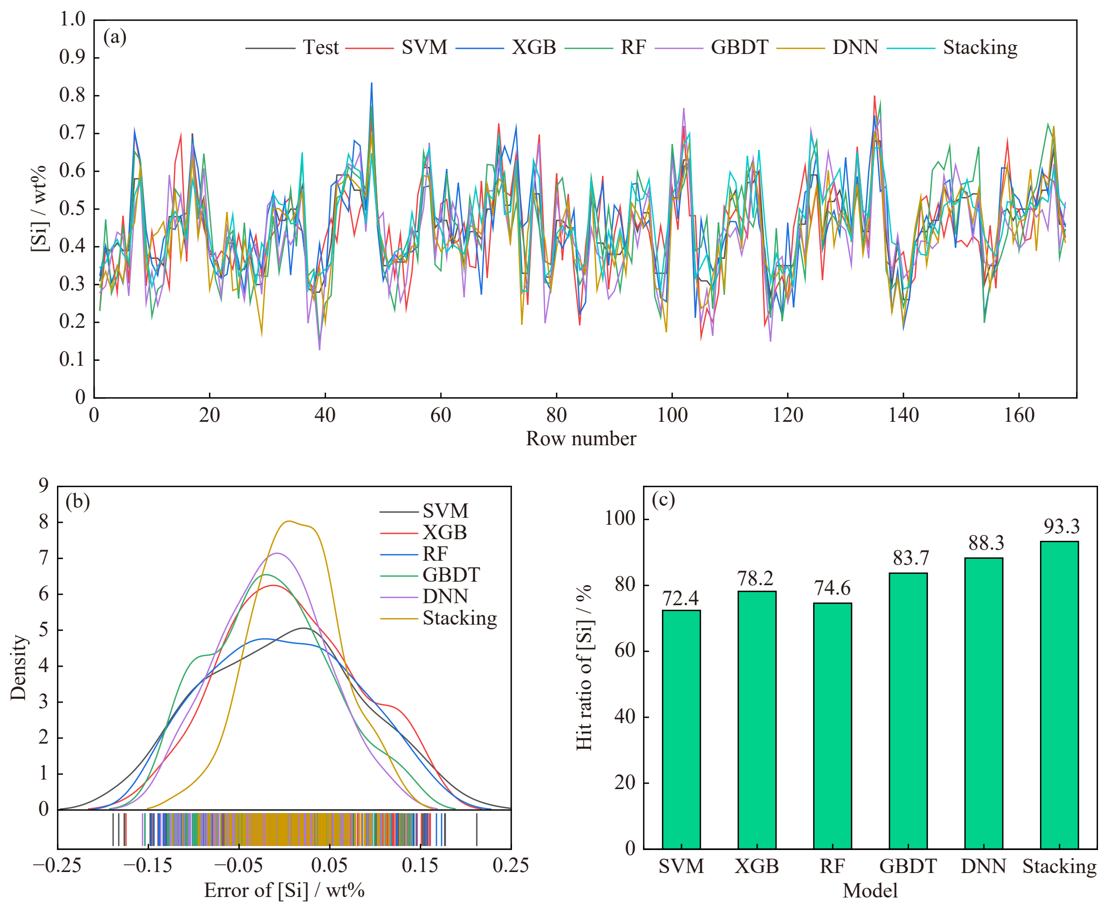


**Fig. 10. Results (a), probability density function (b), and hit ratio (c) of [Si] prediction by different methods.**

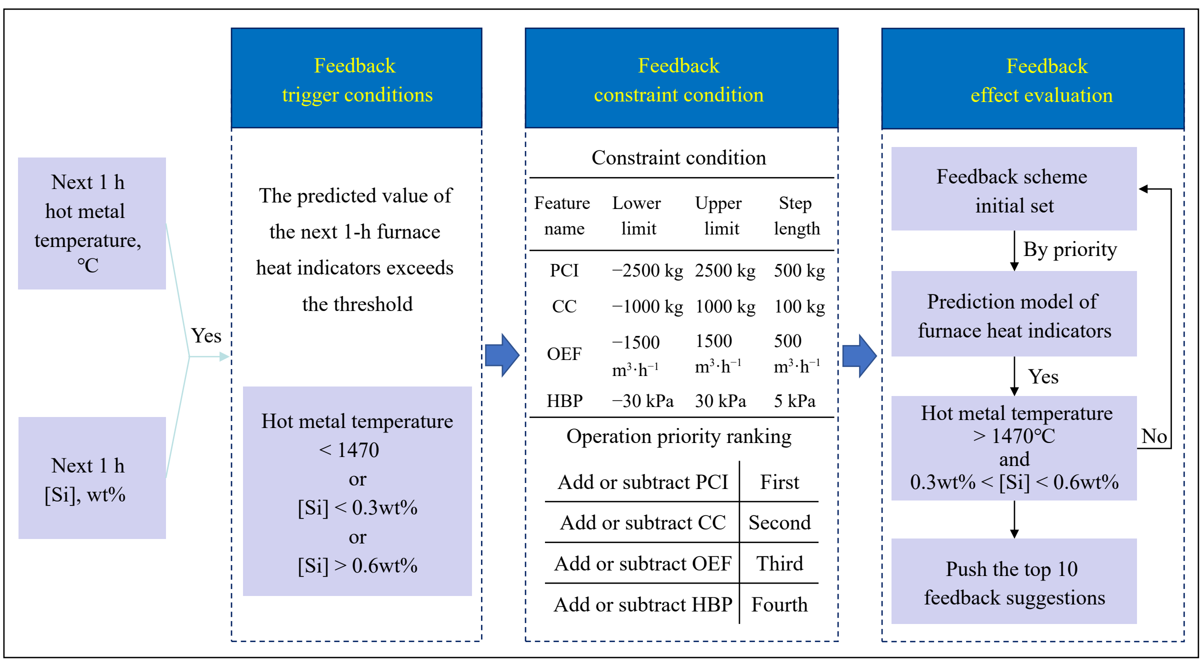


**Fig. 11. Process of the feedback model of BF heat operation.**

condition. The feedback threshold for hot metal temperature is below 1470°C, and the feedback threshold for [Si] is below 0.3wt% or above 0.6wt%. The feedback process was triggered when the predicted result (the next hour) of any furnace heat indicator exceeded the threshold. In the second part, the constraint conditions of feedback adjustment were set in accordance with practical production. These conditions included adjustable parameters and their adjustment range and step size. The adjustable parameters in this work were pulverized coal injection (PCI), coke consumption (CC), oxygen enrichment flow (OEF), and hot blast pressure (HBP). The priority of the adjustment parameters followed the order of PCI, CC, OEF, and HBP. For example, PCI had a lower limit, upper limit, and step size of –2500 kg, 2500 kg, and 500 kg, respectively. In the third part, the final feedback of parameters was provided to the operator. An initial feedback scheme set was established on the basis of adjustment rules, as seen in Table 5. A total of 21020 types of schemes were obtained. Each scheme in the initial feedback scheme set was evaluated by using the prediction model of the furnace heat indicator. The schemes that met the threshold of furnace heat indicators were screened out and sorted in accordance with priority. Finally, the top 10 feedback schemes meeting the optimization objectives of furnace heat indicators were selected and pushed to the BF operator.

3.4.2. Analysis of feedback results

The feedback of furnace heat indicators during the online operation was taken as an example. The current temperature and [Si] were 1464°C and 0.26wt%, respectively, and the predicted values at the following time were 1466°C and 0.28wt%, respectively. Then, the initial feedback scheme was searched, and the top 10 operation suggestions with evaluation results that met the requirements of a temperature above 1470°C and [Si] between 0.3wt% and 0.6wt% were selected and provided. The detailed feedback results are shown in Table 6. The temperature and [Si] were lower than the required range of furnace heat indicators, indicating that the furnace heat level at this time was lower than normal. Therefore, heat must be supplemented to increase the furnace heat level. The operation suggestions of screening were mainly about increasing fuel consumption and were consistent with the purpose of heat supplementation and with the BF smelting theory. At the same time, the operation suggestions were quantitatively pushed. The suggestions were highly useful to the BF operator in restoring furnace heat levels and stabilizing furnace conditions.

### 3.5. Adaptive updates of the model for furnace heat prediction

The BF heat level was obviously affected by the change in raw material and recent furnace conditions. Given that the model was trained with historical data with timeliness, the model parameters must be updated adaptively in accordance with the latest process data. Such an approach will enhance

**Table 5. Initial feedback scheme set**

| No. | PCI adjustment / kg | CC adjustment / kg | OEF adjustment / ($m^3 \cdot h^{-1}$) | HBP adjustment / kPa |
|---|---|---|---|---|
| 1 | −500 | 0 | 0 | 0 |
| 2 | 500 | 0 | 0 | 0 |
| 3 | −1000 | 0 | 0 | 0 |
| 4 | 1000 | 0 | 0 | 0 |
| 5 | −1500 | 0 | 0 | 0 |
| … | … | … | … | … |
| 10001 | −1500 | 600 | 1000 | −15 |
| 10002 | −1500 | 600 | 1000 | 15 |
| 10003 | 1500 | −600 | −1000 | −15 |
| 10004 | 1500 | −600 | −1000 | 15 |
| 10005 | 1500 | −600 | 1000 | −15 |
| … | … | … | … | … |
| 21016 | 2500 | −1000 | 1500 | 30 |
| 21017 | 2500 | 1000 | −1500 | −30 |
| 21018 | 2500 | 1000 | −1500 | 30 |
| 21019 | 2500 | 1000 | 1500 | −30 |
| 21020 | 2500 | 1000 | 1500 | 30 |

**Table 6. Feedback results of the furnace heat model**

| No. | PCI adjustment / kg | CC adjustment / kg | OEF adjustment / ($m^3 \cdot h^{-1}$) | HBP adjustment / kPa | HMT prediction / °C | [Si] prediction / wt% |
|---|---|---|---|---|---|---|
| 1 | 1000 | 300 | 500 | 5 | 1472.40 | 0.35 |
| 2 | 1000 | 200 | 500 | 5 | 1478.42 | 0.38 |
| 3 | 1000 | 300 | 500 | 0 | 1471.12 | 0.39 |
| 4 | 500 | 200 | 0 | 5 | 1476.87 | 0.41 |
| 5 | 1000 | 200 | 500 | 0 | 1481.00 | 0.46 |
| 6 | 500 | 200 | 500 | 0 | 1478.49 | 0.47 |
| 7 | 500 | 200 | 0 | 0 | 1480.87 | 0.41 |
| 8 | 0 | 200 | 0 | 0 | 1472.24 | 0.43 |
| 9 | 1000 | 100 | 0 | 0 | 1473.62 | 0.44 |
| 10 | 500 | 100 | 0 | 0 | 1472.10 | 0.41 |

the production adaptability of the model. An adaptive updating measure was adopted to ensure stable performance, and the superiority and practicability of the proposed method were verified through an online application. The process of adaptive updating is depicted in Fig. 12. The first measure was to update the training set in real time before each prediction on the basis of the hyperparameters of the training model. The latest data were applied to train the model. Then, the online adaptive updating of the model, which had the advantage of satisfying the response speed of the online application and extending the timeliness of the model to a certain extent, was finally realized. The second measure was periodic adaptive renewal. When the average hit ratio of the model was lower than 85% in one week, the input features and metaparameters of the model were completely updated according to the latest accumulated historical data to ensure the stable performance of the model. This process took a long time and was completed in a new process without affecting the online running of the model. The furnace heat indicator model was successfully self-updated six times, as seen in Fig. 13. Red represents the hit ratio of the model before updating (<85%), and green represents the hit ratio of the model after updating. Evidently, the hit ratio of the model gradually declined over time but significantly improved after each self-updating and can meet production requirements.

## 4. Practical application

On the basis of the results of this work, a BF heat prediction and feedback system was developed and successfully applied online to an ongoing BF in China. This system, which is illustrated, included two modules: the tracking of input data and the prediction of heat indicators and feedback of operation suggestions. This system ran stably and achieved remarkable economic benefits over 1 year of application. The hit ratio of the dynamic prediction of furnace heat indicators within 24 h exceeded 95% for a long time, and the feedback of operation suggestions, which had played an important role in stabilizing the furnace condition, was highly accepted by BF operators. The expected target of increasing the furnace

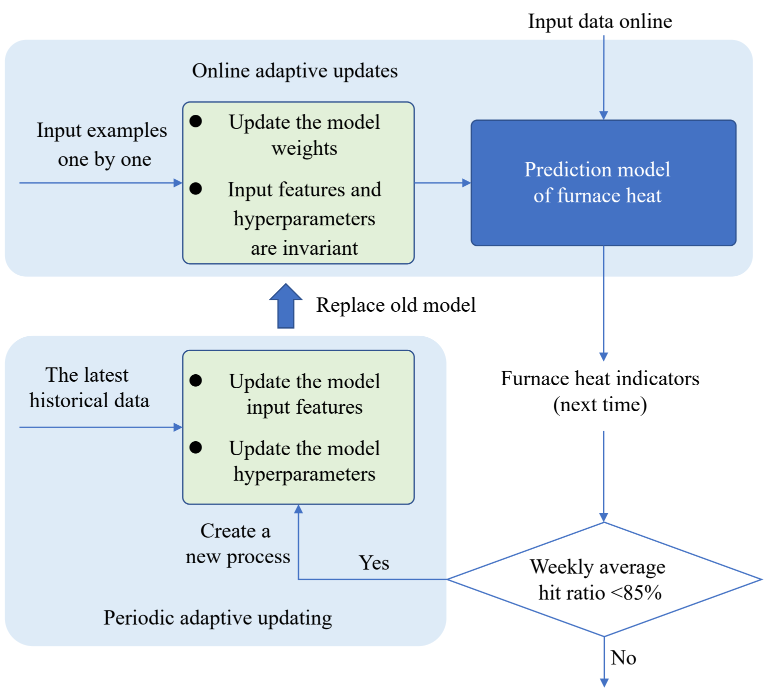


**Fig. 12. Process of adaptive updating.**

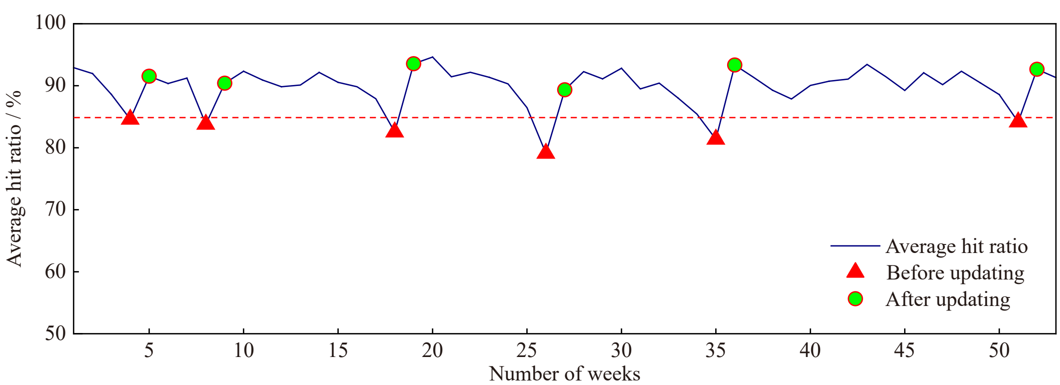


**Fig. 13. Statistical results of model self-updating.**

temperature stability rate from 54.9% to 84.9%, which represented an increase of 30%, was reached.

## 5. Conclusions

(1) The data, which included data on raw materials, fuel and process operation, smelting state, and slag and iron discharge during the whole BF ironmaking process, were analyzed. It included 171 variables and 9223 sets of data. Data quality was effectively improved through data governance. The time delay relationship between relevant variables and furnace heat indicators was fully considered and played an important role in establishing the scientific prediction model.

(2) The furnace heat prediction model was established on the basis of GA and stacking frameworks. This approach was conducive to improving the performance instability of a single machine learning algorithm on different datasets effectively. The performance of the proposed method was verified through comparison with five other machine learning algorithms. The hit ratio of temperature within the error range of ±10°C and [Si] within the error range of ±0.1wt% were 92.4% and 93.3%, respectively. These values can meet the requirements of practical production.

(3) The furnace heat feedback model conforming to BF was successfully established. Operation suggestions were quantitatively pushed and were highly accepted by BF operators. In addition, the system of furnace heat prediction and feedback was successfully applied. The furnace temperature level improved obviously during the application period. The dynamic prediction hit ratio of the furnace heat indicator within 24 h exceeded 95% for a long time. The expected target of increasing the furnace temperature stability rate from 54.9% to 84.9%, which represented an increase of 30%, was reached.

## Acknowledgements

This research was financially supported by the General Program of the National Natural Science Foundation of China (No. 52274326), and the Fundamental Research Funds for the Central Universities (No. N2425031), and Seventh Batch of Ten Thousand Talents Plan (No. ZX20220553), and China Baowu Low Carbon Metallurgy Innovation Foundation (No. BWLCF202109), and The key technology research and development and application of digital transformation throughout the iron and steel production process (No. 2023JH2/101800058), and Liaoning Province Science and Technology Plan Joint Program (Key Research and Development Program Project).

## Conflict of Interest

Mangsheng Chu is an editorial board member for this journal and was not involved in the editorial review or the decision to publish this article. All authors declare that there are no competing interests.

## References

[1] D. Pan, Z.H. Jiang, Z.P. Chen, W.H. Gui, Y.F. Xie, and C.H. Yang, Temperature measurement method for blast furnace molten iron based on infrared thermography and temperature reduction model, *Sensors*, 18(2018), No. 11, art. No. 3792.

[2] X. Liu, W.J. Zhang, Q. Shi, and L. Zhou, Operation parameters optimization of blast furnaces based on data mining and cleaning, *J. Northeastern Univ. Nat. Sci.*, 41(2020), No. 8, p. 1153.

[3] Z.N. Li, M.S. Chu, Z.G. Liu, G.J. Ruan, and B.F. Li, Furnace heat prediction and control model and its application to large blast furnace, *High Temp. Mater. Process.*, 38(2019), p. 884.

[4] X.J. Liu, Y. Deng, X. Li, L.Y. Hao, E.H. Liu, and Q. Lyu, Prediction of silicon content in hot molten of blast furnace based on bid data technology, *China Metall.*, 31(2021), No. 2, p. 10.

[5] M.S. Chu, J. Yagi, and F. Shen, *Modelling on Blast Furnace Process and Innovative Ironmaking Technologies*, Northeastern University Press, Shenyang, 2006, p.36.

[6] X.G. Liu and F. Liu, *Blast Furnace Ironmaking Process Optimization and Intelligent Control system*, Metallurgy Industry Press, Beijing, 2003, p. 90.

[7] Q. Shi, J. Tang, and M.S. Chu, Key issues and progress of industrial big data-based intelligent blast furnace ironmaking technology, *Int. J. Miner. Metall. Mater.*, 30(2023), No. 9, p. 1651.

[8] R.Y. Yin, Review on the study of metallurgical process engineering, *Int. J. Miner. Metall. Mater.*, 28(2021), No. 8, p. 1253.

[9] Q. Shi, J. Tang, and M.S. Chu, Evaluation, prediction, and feedback of blast furnace hearth activity based on data-driven analysis and process metallurgy, *Steel Res. Int.*, 95 (2024), art. No. 2300385.

[10] G.F. Pan, F.Y. Wang, C.L. Shang, *et al.*, Advances in machine learning- and artificial intelligence-assisted material design of steels, *Int. J. Miner. Metall. Mater.*, 30(2023), No. 6, p. 1003.

[11] R.H. Zhang and J. Yang, State of the art in applications of machine learning in steelmaking process modeling, *Int. J. Miner. Metall. Mater.*, 30(2023), No. 11, . 2055.

[12] C.L. Huang, Y.L. Tang, X.F. Zhang, and Y.Z. Chu, Prediction and simulation of silicon content in blast furnace for PCA and PSO–ELM, *Comput. Simul.*, 37(2020), No. 2, p. 398.

[13] M. Yuan, P. Zhou, M.L. Li, R.F. Li, H. Wang, and T.Y. Chai, Intelligent multivariable modeling of blast furnace molten iron quality based on dynamic AGA-ANN and PCA, *J. Iron Steel Res. Int.*, 22(2015), No. 6, p. 487.

[14] P. Zhou, M. Yuan, H. Wang, Z. Wang, and T.Y. Chai, Multivariable dynamic modeling for molten iron quality using online sequential random vector functional-link networks with self-feedback connections, *Inf. Sci.*, 325(2015), p. 237.

[15] Z.Y. Wang, D.H. Jiang, X.D. Wang, J.L. Zhang, Z.J. Liu, and B.J. Zhao, Prediction of blast furnace hot metal temperature based on support vector regression and extreme learning machine, *Chin. J. Eng.*, 43(2021), No. 4, p. 569.

[16] J.P. Li, C.C. Hua, and X.P. Guan, Inputs screening of hot metal silicon content model on blast furnace, [in] *2017 Chinese Automation Congress* (*CAC*), Jinan, 2017, p. 3747.

[17] Y. Deng and Q. Lyu, Establishment of evaluation and prediction system of comprehensive state based on big data technology in a commercial blast furnace, *ISIJ Int.*, 60(2020), No. 5, p. 898.

[18] P. Zhou, P. Dai, H.D. Song, and T.Y. Chai, Data-driven recursive subspace identification based online modelling for prediction and control of molten iron quality in blast furnace ironmaking, *IET Control Theory Appl.*, 11(2017), No. 14, p. 2343.

[19] Y.R. Li and C.J. Yang, Domain knowledge based explainable feature construction method and its application in ironmaking process, *Eng. Appl. Artif. Intell.*, 100(2021), art. No. 104197.
[20] K. Jiang, Z.H. Jiang, Y.F. Xie, D. Pan, and W.H. Gui, Prediction of multiple molten iron quality indices in the blast furnace ironmaking process based on attention-wise deep transfer network, *IEEE Trans. Instrum. Meas.*, 71(2022), art. No. 2512114.
[21] J.P. Li, C.C. Hua, Y.N. Yang, and X.P. Guan, A novel MIMO T–S fuzzy modeling for prediction of blast furnace molten iron quality with missing outputs, *IEEE Trans. Fuzzy Syst.*, 29(2021), No. 6, p. 1654.
[22] J.P. Li, C.C. Hua, and Y.N. Yang, A novel multiple-input–multiple-output random vector functional-link networks for predicting molten iron quality indexes in blast furnace, *IEEE Trans. Ind. Electron.*, 68(2021), No. 11, p. 11309.
[23] J.P. Li, C.C. Hua, J.L. Qian, and X.P. Guan, Low-rank based Multi-Input Multi-Output Takagi-Sugeno fuzzy modeling for prediction of molten iron quality in blast furnace, *Fuzzy Sets Syst.*, 421(2021), p. 178.
[24] Z.N. Li, *Prediction and Optimization of Key Process Parameters of Large Blast Furnace Based on Big Data Mining* [Dissertation], Northeastern University, Shenyang, 2020, p. 27.
[25] Y. Han, Z.B. Hu, A.M. Yang, J. Li, and Y.Z. Zhang, Intelligent recommendation model for reducing silicon deviation fluctuation of hot metal in BF and application, *Iron Steel*, 58(2023), p. 30.
[26] H.Y. Li, X.P. Bu, X.J. Liu, *et al*., Evaluation and prediction of blast furnace status based on big data platform of ironmaking and data mining, *ISIJ Int.*, 61(2021), No. 1, p. 108.
[27] J.L. Bai, J.L. Zhang, H.W. Guo, S. Du, and Y.J. Cao, Basic mathematical models in blast furnace expert system, *J. Wuhan Univ. Sci. Technol.*, 36(2013), No. 5, p. 331.
[28] J.L. Zhang, X.D. Jiang, H.B. Zuo, and Z.J. Liu, Heat state judgment for calcium carbide furnaces based on heat index calculation and furnace temperature prediction, *Chin. J. Eng.*, 35(2013), No. 9, p. 1131.
[29] L. Wei, S.S. Yang, F. Zhang, and Q. Bai, A Mathematical model on prediction of hot metal silicon content and temperature using blast furnace hearth thermal state parameters, [in] *Metallurgical Research Center 2005 Metallurgical Engineering Science Forum*, Beijing, 2005, p. 62.
[30] X.Q. Niu, Q.W. Ye, Y. Zhou, and X.D. Wang, Autoregressive model electroencephalogram signal identification based on feature selection of genetic algorithm, *Comput. Eng.*, 42(2016), No. 3, p. 283.
[31] Z.Q. Li, J.Q. Du, B. Nie, W.P. Xiong, C.Y. Huang, and H. Li, Summary of feature selection methods, *Comput. Eng. Appl.*, 55(2019), No. 24, p. 10.
[32] H.B. Yu, Q.N. Zhu, L. Kang, G.Z. Qiao, and J.C. Zeng, A Multi-operator collaborative particle swarm optimization algorithm with biased roulette, *Control Decis.*, 39(2024), No. 4, p. 1167.
[33] J.W. Xu and Y. Yang, A survey of ensemble learning approaches, *J. Yunnan Univ. Nat. Sci. Ed.*, 40(2018), No. 6, p. 1082.
[34] Z.N. Li, M.S. Chu, Z.G. Liu, and B.F. Li, Prediction and optimization of blast furnace parameters based on machine learning and genetic algorithm, *J. Northeastern Univ. Nat. Sci. Ed.*, 41(2020), No. 9, p. 1262.
[35] Q. Feng, Q. Li, W. Quan, and X.M. Pei, Overview of multiobjective particle swarm optimization algorithm, *Chin. J. Eng.*, 43(2021), No. 6, p. 745.